HiSST: International Conference on
High-Speed Vehicle Science Technology
26–29 November 2018, Moscow, Russia

The Research of Features of the Flow Structure in a Multichannel Supersonic Air Intake.

Dmitry A. Rakhmanin[1], Alexander K.Trifonov[2]

Abstract

When considering multichannel air intake devices, it is necessary to take into account a set of flow features that distinguish them from conventional single-channel air intake devices. The results of computational and experimental studies of the flow characteristics in the channels of the air intake device consisting of four channel inlets operating on a single chamber are presented. The object of research is single-mode four-channel air intake devices designed for small supersonic speeds corresponding to the Mach number M=1,8. The flow structure in the channel of each inlet, which changes during the mechanical throttling of the entire air intake device, is considered. It is shown experimentally that the difference between the highest and lowest values of the total pressure recovery coefficient in the channels of the air intake device in the area of the angular point of throttle characteristic can reach a significant value. The influence of vortexes formed in the end part of the integration chamber on the operation resistance of the air intake device is considered, and a possible way to increase the stability of the intake is considered.

Key words: *air intake device, throttle characteristic, vortex flow, aerophysical experiment, numerical simulation.*

Nomenclature

Latin

E – total energy mass density
F – inviscid flux vector
F_0 – area of the intake inlet
F_c – measuring nozzle critical section area
F_{ch} – cross section area of the channel
F_f – cross sectional area of the captured by the intake airflow in the free stream
F_{th} – the throttle area
G – viscous flux vector
H – the vector of source terms
L – length of the channel
M – Mach number
P – static pressure
$P_{0,\infty}$ – the total pressure of free-stream flow
$P_{0,c}$ – total pressure critical section of the measuring nozzle
$P_{0(en)}$ – the total pressure of stagnated air in front of the engine
P_{0i} – total pressure in the probe "i"
Re – Reynolds number
V – the cell volume
WT – wind tunnel

a – angle of attack
f – mass flow rate
$q(\lambda_c)$ – gas-dynamic function in the measuring nozzle critical section
$q(M_\infty)$, $q(\lambda_\infty)$ – gas-dynamic functions in free stream
u,v,w – velocity components

Greek

ν – the total pressure recovery coefficient
ρ – mass density

[1] *Central Aerohydrodynamic Institute (TsAGI)*
Zhukovsky Street 1, Zhukovsky, Moscow Region, 140180, Russian Federation
[2] *TsAGI, Zhukovsky Street 1, Zhukovsky, Moscow Region, 140180, Russian Federation*

Introduction

When developing multi-channel air intake devices, it is necessary to take into account a number of flow features, which distinguish them from general air intake devices with one channel. The air intake device must provide high performance and gas-dynamic stability of the power plant throughout the required range of numbers M, angles of attack and sideslip, and at Mach numbers close to the maximum when the anti-surge reserves of the air intake device are minimal. The most important subject of the research is to study features of the flow in the channels of the air intake device consisting from several intakes with rectangular inlets operating on one chamber and to determine the flow characteristics in the channel of each air intake during throttling of the entire air intake device taking into account the shape of the gas generator in the combustion chamber.

1. Features of experimental studies

The design of the experimental model of the air intake device with four intakes for a ramjet engine with a gas-generator [1] is presented at Fig.1. The feature of such configurations is the presence of a mixing chamber, in which four channels, and hence four flows, join together. Besides, there is an axisymmetric end surface in the chamber simulating a nonrunning gas-generator.

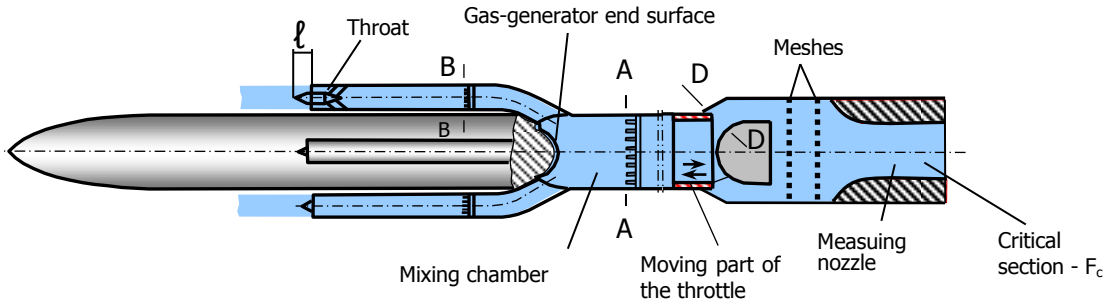

Fig.1. A typical scheme of the experimental setup for the study of the internal characteristics of the air intake device

A series of experimental studies of air intake devices with rectangular inlets was conducted in wind tunnel TSAGI SVS-2 at Mach number M=1.8-2.2. During the experiment, the models were installed on a special holder equipped with a throttle-flow device. After the WT started and stationary regime of flow became established, mechanical throttling (air flow rate variation) of the intake was performed with the throttle-flow device of the holder and all the measured quantities were registered. The experimental equipment of the WT makes it possible to detect the measurements both while opening and closing of the throttle. The air intake throttle characteristic (the dependence of the total pressure recovery coefficient ν from the mass flow rate f) was determined according to the aerometric measurements.

The total pressure recovery coefficient is defined as a ratio of the total pressure of stagnated air in front of the engine $P_{0(en)}$ to the total pressure of free-stream flow $P_{0,\infty}$ (Eq.1):

$$\nu = \frac{P_{0(en)}}{P_{0,\infty}} \tag{1}$$

During the experimental research the total pressure is determined by the Pitot comb placed in front of the combustor inlet of the ramjet engine (section A-A, Fig.1), as well as in the channel of each intake (section B-B, Fig.1).

The mass flow rate of the intake f, equal to the ratio of cross sectional area F_f of the captured by the intake airflow in the free stream to the intake inlet area F_0, is defined from the air flow rate equation written for the section of free stream, incoming the intake, and the critical section of the measuring nozzle (Eq.2):

$$f = \frac{F_f}{F_0} = \frac{P_{0,c} \times q(\lambda_c) \times F_c}{P_{0,\infty} \times q(\lambda_\infty) \times F_0}, \quad (2)$$

where F_c, F_0 – measuring nozzle critical section area and intake inlet area, respectively,

$P_{0,c}$, $P_{0,\infty}$ – total pressure in front of the measuring nozzle and free stream total pressure,

$q(\lambda_c)$, $q(\lambda_\infty)$ – gas-dynamic functions, calculated from the ratio of static and total pressure values in the measuring nozzle critical section and in free stream, respectively.

The total pressure $P_{0,c}$ measurements in front of the measuring nozzle are made by means of the rake with Pitot tubes. The Mach number in the channel of each intake is determined from the ratio of static and total pressure values for each Pitot tube using gas-dynamic functions. At subsonic speeds the dependence of the Mach number from the ratio of static and total pressure values is used, whereas at supersonic speeds the dependence of the Mach number from the ratio of static pressure to total pressure behind the normal shock wave is used. When processing the experimental data, the value of the throttle area F_{th} is used, which is determined from the flow rate equation (Eq.3):

$$\frac{F_{th}}{F_0} = \frac{f \times q(M_\infty)}{\nu_{A\text{-}A}} \quad (3)$$

2. Flow structure in the intake channels while throttling

Experimental research of 4-channel air intake showed, that throttle characteristic of each intake differs from the others by the largest value of total pressure recovery coefficient (Fig.2).

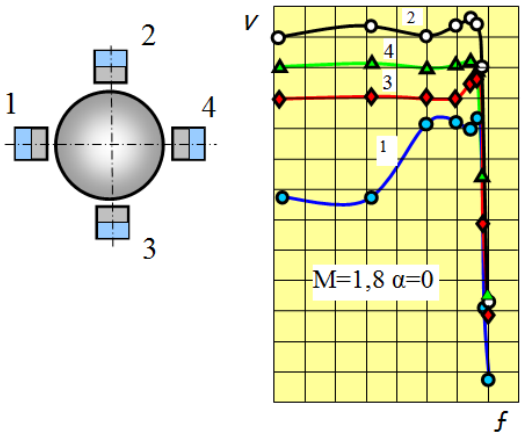

Fig.2. Throttle characteristic of the air intake channels

The graph on the Fig.2. for rectangular inlets shows, that the largest value of the coefficient ν occur in the channel 2, and the least value – in the channel 1. In the region of the corner point the difference can reach $\Delta\nu = 11\%$.

Let's move to a more detailed flow analysis in rectangular channels of the air intake. A vertical rake with 5 probes was mounted in each channel (enumeration P_{0i} was held from inner wall of the channel to its outer wall). The Fig.3 demonstrates the ratio of the average values of static pressure to the total pressure of the incoming flow $P/P_{0,\infty}$ in each channel, depending on the degree of throttling, namely, the conditional area of the throttle – F_{th}. The graph also shows the limit of the throttle area F_{th} separating the supersonic flow from the subsonic, determined on the basis of the measured values of static and total pressures.

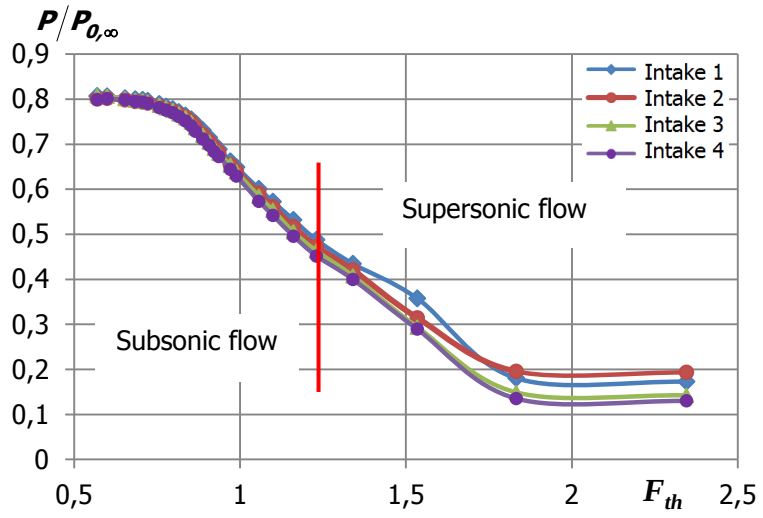

Fig.3. Dependence of the pressure ratio $P/P_{0,\infty}$ on the throttle area. $M = 1.8, \alpha = 0$

The values of ratio of total pressure in each probe to the total pressure of free-stream flow $P_{0i}/P_{0,\infty}$ for four resulting readings at angular point of throttle characteristic were compared. The largest and the least values of this ratio for each channel are represented on the Fig.4 and marked as $\nu_{\max}$ and $\nu_{\min}$, respectively.

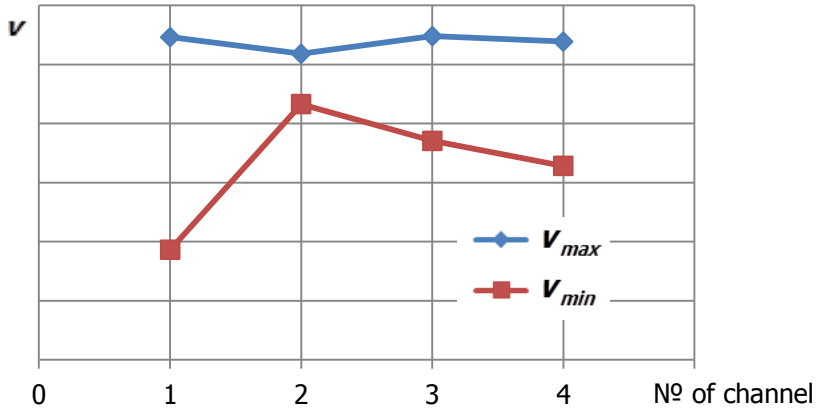

Fig.4. The values ν_{max} and ν_{min} in the angular point of the throttle characteristic for different channels. $M = 1.8, \alpha = 0$

The ratio of static pressure to total pressure for all probes in every channel P/P_{0i} versus throttle area F_{th} from totally opened to the value $F_{th} = 1.34$ is presented on the Fig.5. The total pressure fields represented on the Fig.5 suggest that it is possible to divide the flow along the height of the rake into three flows - the main stream and the vortex flows along the sides of the main flow. The Fig.4 shows the values of total pressure recovery coefficient in the corner point of throttle characteristic for the main flow – $\nu_{\max}$ and the same coefficient in vortex flows – $\nu_{\min}$.

It may be assumed that the main flow features high values of total pressure $\nu_{\max}$, which correspond to standard values. It should be noticed that all the values $\nu_{\max}$ are on the same level. Vortex flows are characterized by low values of pressure $\nu_{\min}$. The main feature is that the values $\nu_{\min}$ in different channels vary widely. Hence, the difference between total pressure fields is defined by the pressure value in vortex layer. The lowest values $\nu_{\min}$ occur in the first channel, and the highest – in the second one.

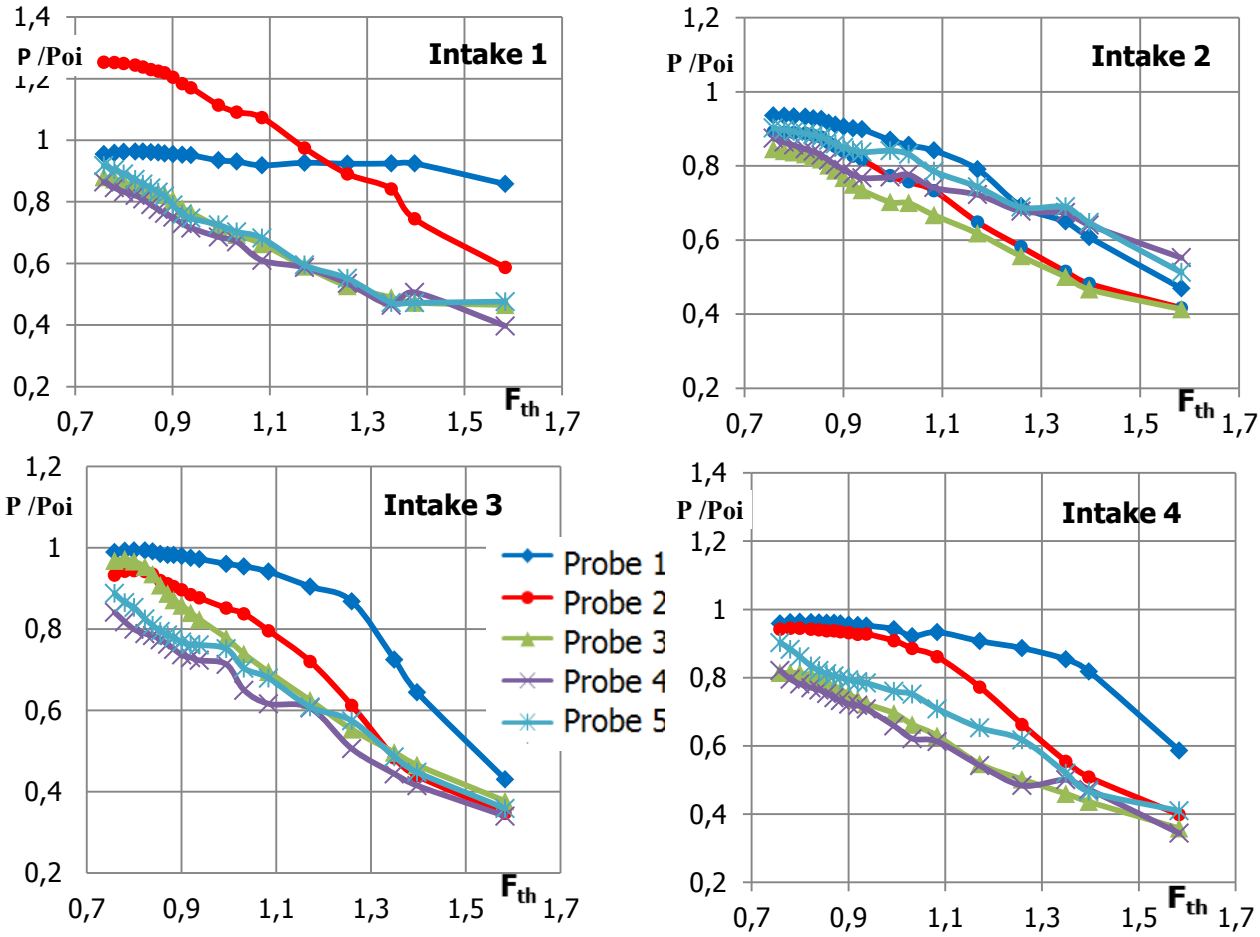

Fig.5. The P/P_{oi} versus throttle area in the intake channels diagram

The Fig.5 shows, that the probe 2 in the 1st channel at $F_{th} < 1.18$ detects the value, which is higher than one $(P/P_{oi} > 1)$, that reveals the formation of vortex flow zone. The height of this zone may extend over 2/3 of the channel height. In all the other intakes the value P/P_{oi} is lower than one. While throttling the vortex zone goes upstream that corresponds to the pseudoshock migration.

In the intake 1 the main stream is located between probes 3 and 5, and the main vortex flow is between the probe 3 and the channel wall close to the probe 1. Therefore the main vortex flow occupies a half of the channel. The thickness of vortex flow near the opposite wall is far smaller, it is situated between the probe 5 and the channel wall. As a whole, the vortex flow in the intake 1 can occupy more than a half of its channel. Conversely, in the intake 2 the main vortex flow is situated near the probe 4, and the main stream is almost in the center of the channel. In other words, the flow structure is close to symmetric relating to the channel axis.

3. Numerical simulation

To conduct a more thorough analysis of the flow in the channels of the air intake device, a numerical simulation was carried out using the CFD-FASTRAN program code (Costumer № 2482) from ESI-GROUP [2-6].

The used numerical scheme is finite-volume Rieman solver with the upstream difference scheme for spatial derivative calculation. The following Navier-Stokes equations (Eq.4) are solved using the finite volume method:

$$\int \frac{\partial \vec{Q}}{\partial t} dV + \int \nabla \times \vec{F}^{n+1} dV = 0 \,, \tag{4}$$

where the vector $Q = (\rho, \rho u, \rho v, \rho w, E)$;the tensor $\vec{F} = (F, G, H)$ and where F and G are inviscid and viscous flux vectors, respectively, H is the vector of source terms, V is the cell volume.

The flow solution is completed with the use of Roe scheme with the second-order accuracy. In order to speed up the solution the fully-implicit integration scheme with dual time step providing global time accuracy with time step equal 1,0e-007 sec is used. For the concerned speed range the Reynolds numbers vary within $\mathrm{Re} = 2 \div 4 \cdot 10^6$, thus, the Navier-Stokes equations are enclosed by SST turbulence model. The main equations imply a number of connected nonlinear equations with partial derivatives. They should be discretized for being solved numerically. Spatial discretization of the problem is performed by splitting of the computational domain at little contacting volumes. There is one (and only one) junction point inside every volume. Grid cells are used as a control volume: grid points are located in vertexes of polyhedron (for structured grids – hexahedron), grid lines pass along its edges, and the required values are assigned to the geometric cell center of the desirable mesh solution. Creation of high-quality mesh is the key point in such kind of flow simulation. Thus, the entire computational domain forms a multiblock structure. It should be noticed that it was selected about 40 cells for the boundary layer with their orthogonalization near the surface, and as a result the sum of grid points was about 18 mil.

Computational flow picture of the throttled down channel is presented on the Fig.6. It shows that the pseudoshock location is different in the upper and in the lower channel. It is caused by unsymmetrical flow around the end surface of gas-generator relating the central vertical plane. Also there is a zone of separated flow at the lower surface of the channel, and its height reaches about 1/3 of the channel height.

To sum up, the total pressure fields in the intakes differ from each other during throttling. Thus, arithmetical averaging of ν results in difference of throttle characteristic and in loss of accuracy of total pressure recovery coefficient determination, and therefore, of throttle characteristic. Besides, the mentioned flow distortion doesn't allow to define the mass flow through each intake. Inaccuracy of determination can reach 40%. However, regardless this fact it is still possible to define the channel, in which the leading wave appears earlier, than it the others.

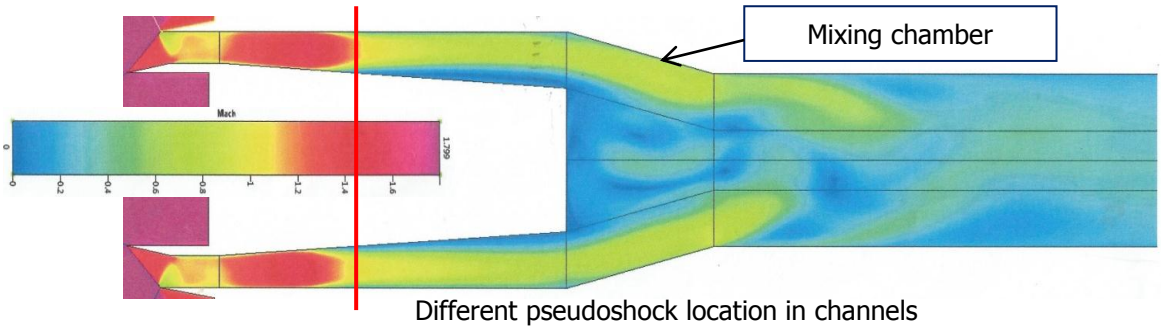

Fig. 6. Numerical simulation. Vortex flow in the mixing chamber. *M = 1.8, α = 0*

The Fig.6. represents the flow around the end surface of the mixing chamber. There are a lot of vortexes of different size behind the end surface, moreover, they "move away" the main stream while throttling. It should be noticed that the flow around the end surface is locally unsteady, in other words, the configuration and size of vortexes vary through time inside stable recirculating zone.

Dissimilarity of flow structure in different channels is derived from flow junction in the mixing chamber. The cross sectional area of mixing chamber is considerably larger than total area of channels (Fig. 7a), and there is situated the gas-generator end surface that can cause vortex flow formation. It may be assumed that throttling leads to formation of distortion in the channel, as the

same supersonic flow is realized in all channels in the case of free inflow into the common cavity. However, the flow separation moves from the end surface to the lower surface of rectangular channels as far as backward pressure reaches the end surface and interacts with the recirculating zone.

Computer simulation proved the fact that complex vortex flow forms in the mixing chamber. The reason of longitudinal vortex formation at the channels exit is high area differential, as there is instantaneous expansion of the channels through transformation into cylindrical integration chamber.

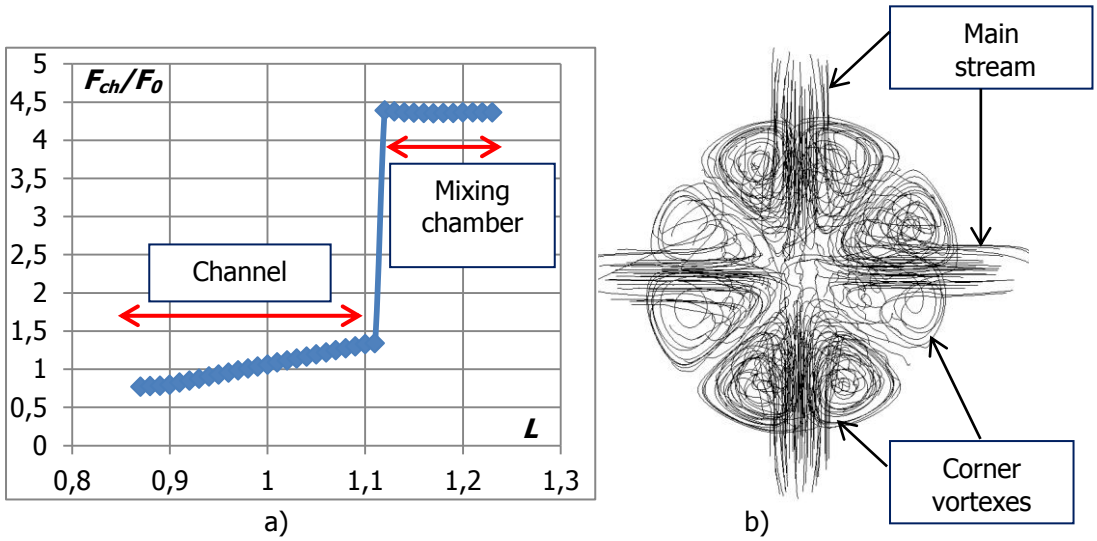

Fig. 7. Numerical simulation. a) area variation along the length of the channel, b) streamlines in the mixing chamber. *M = 1.8, α = 0*

The Fig.7b shows computational flow structure in the cross-section right after the section of streams inflow into the mixing chamber. Studies showed that right after this section the stream as it leaves the channel expands into three directions, that is the volume between channels and towards the mixing chamber axis, flowing round the gas-generator end surface. As a consequence (Fig.7b) two side vortexes and one main stream flow appear behind each channel. Downstream two side vortexes approach and the main stream flow deflects to the center. Similar results were achieved in [7].

As is shown above, the key aspect of the flow in different channels is that throttling cause formation of separated flows of different configuration on surfaces of the channels. These flows in their turn lead to further pressure changes in channel, thus accelerating the pseudoshock motion. Vortex structure in the mixing chamber is very sensitive to minor variation of channel geometry downstream of it. The vortex reacts on small disturbances and changes its own form under their influence.

In order to estimate the influence of end surface shape on recirculating zone size, the mounting of cone frustum in the end surface of mixing chamber was modeled. The Fig.8 shows that the presence of cone frustum changes the flow pattern in the mixing chamber significantly. It was found that the separation zone moved to the opposite wall of the channel (Fig.8).

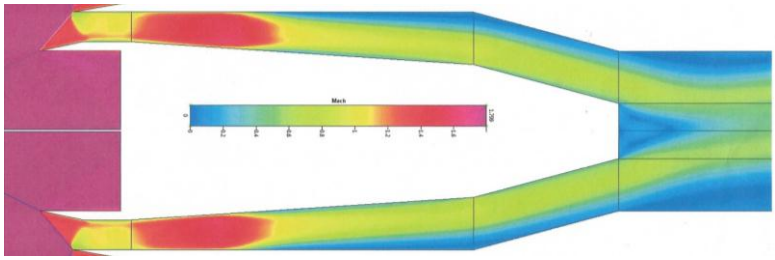

Fig. 8. The influence of the truncated cone on the flow in the channels

Thus, the decrease in the area difference leads to the decrease or elimination of the separation zone on the lower wall of the rectangular channel. However, it should be noticed that it is apparently necessary to make not only longitudinal, but also transverse channel profiling in order to eliminate flow separation from the upper part of the channel.

Conclusion

On the basis of the obtained experimental and simulation studies of the four-channel air intake device, it was found that the total pressure fields for each channel differ when throttling. In the area of the angular point this difference can reach $\Delta v = 11\%$. The non-synchronous throttling of the channels is caused by the flow field features in the mixing chamber, in which four streams of the flow join together.

When throttling, separated flows of different shapes are formed on the surface of the channels; this lead to additional pressure changes in the channel, thereby accelerating the upstream movement of the pseudoshock. The marked unsteadiness allows us to determine the channel, in which the leading wave occurs earlier than in the others.

It is shown that the decrease in the area difference in the mixing chamber leads to the decrease or elimination of the separation zone on the lower wall of rectangular channels. In the meantime, a separation zone appears on the upper wall of the channels. Therefore, in order to eliminate flow separation from the upper part of the channel, apparently, it is necessary to make not only longitudinal, but also transverse channel profiling.

References:

1. Sorokin, V. A., Yanovsky, L. S., Kozlov, Surikov, E. V., and other Rocket engines with solid and paste fuels. - Moscow: Fizmatlit, 2010. 320 PP.

2. Chen L., Tao C.C. Study of the Side — Inlet Dump Combustor of Solid — Ducted Rocket with Reacting Flow // AIAA Paper, 1984. №1378.

3. Cherng D. L., Yang V., Kuo K. Theoretical Study of Turbulent Reacting Flow in a Solid-Propellant Ducted Rocket Combustor // AIAA Paper, 1987. №1723.

4. Hong Z.-C., Chung-Li, Tzu-Hsiang Ko.A Numerical Study on the ThreeDimensional Vortex Motion in a Side-Inlet Dump Combustor // AIAA Paper, 1988. №3009.

5. Liou T.-M., Hwang Y.-H., Hung Y.-Computational Study of Flow Field in Side-Inlet Ramjet Combustors // AIAA Paper, 1988. №3010.

6. Cherng D. L. Yang H. T., Kuo J. Numerical Simulation of Complex Reacting Flows in a Hybrid Ramjet Combustor // AIAA Paper, 1990. №2070.

7. T. Le Pichon T., Laverdant A. Numerical Simulation of Reactive Flows in Ramjet Type Combustors and Associated Validation Experiments // AerospaceLab journal, 2016. AL11-03.